Journal of Hepatocellular Carcinoma

Dovepress
open access to scientific and medical research

Open Access Full Text Article

ORIGINAL RESEARCH

CT-Based Radiomics for the Recurrence Prediction of Hepatocellular Carcinoma After Surgical Resection

Fang Wang[1,*], Qingqing Chen[1,*], Yuanyuan Zhang[1,2], Yinan Chen[3], Yajing Zhu[3], Wei Zhou[4], Xiao Liang[5], Yunjun Yang[6], Hongjie Hu[1]

[1]Department of Radiology, Sir Run Run Shaw Hospital, Zhejiang University School of Medicine, Hangzhou, 310016, People's Republic of China; [2]Medical College, Shaoxing University, Shaoxing, 312000, People's Republic of China; [3]SenseTime Research, Shanghai, 200030, People's Republic of China; [4]Department of Radiology, Huzhou Central Hospital, Affiliated to Huzhou University, Huzhou, 313000, People's Republic of China; [5]Department of General Surgery, Sir Run Run Shaw Hospital, Zhejiang University School of Medicine, Hangzhou, 310016, People's Republic of China; [6]Department of Radiology, The First Affiliated Hospital, Wenzhou Medical University, Wenzhou, People's Republic of China

*These authors contributed equally to this work

Correspondence: Hongjie Hu, Department of Radiology, Sir Run Run Shaw Hospital, Zhejiang University School of Medicine, Hangzhou, 310016, People's Republic of China, Tel/Fax +86-0571-86044817, Email hongjiehu@zju.edu.cn; Yunjun Yang, Department of Radiology, The First Affiliated Hospital, Wenzhou Medical University, Wenzhou, People's Republic of China, Email greatham26@163.com

Purpose: To explore the effectiveness of radiomics signature in predicting the recurrence of hepatocellular carcinoma (HCC) and the benefit of postoperative adjuvant transcatheter arterial chemoembolization (PA-TACE).

Patients and Methods: In this multicenter retrospective study, 364 consecutive patients with multi-phase computed tomography (CT) images were included. Recurrence-related radiomics features of intra- and peritumoral regions were extracted from the pre-contrast, arterial and portal venous phase, respectively. The radiomics model was established in the training cohort (n = 187) using random survival forests analysis to output prediction probability as "Rad-score" and validated by the internal (n = 92) and external validation cohorts (n = 85). Besides, the Clinical nomogram was developed by clinical-radiologic-pathologic characteristics, and the Combined nomogram was further constructed to evaluate the added value of the Rad-score for individualized recurrence-free survival (RFS) prediction, which is our primary and only endpoint. The performance of the three models was assessed by the concordance index (C-index). Furthermore, all the patients were stratified into high- and low-risk groups of recurrence by the median value of the Rad-score to analyze the benefit of PA-TACE.

Results: The model built using radiomics signature demonstrated favorable prediction of HCC recurrence across all datasets, with C-index of 0.892, 0.812, 0.809, separately in the training, the internal and external validation cohorts. Univariate and multivariate analysis revealed that the Rad-score was an independent prognostic factor. Significant differences were found between the high- and low-risk group in RFS prediction in all three cohorts. Further analysis showed that compared with the low-risk group, patients with the high-risk received more benefits from PA-TACE.

Conclusion: The newly developed Rad-score was not only a powerful biomarker in predicting the RFS of HCC but also a strong stratification basis to explore the high-risk patients who could benefit from PA-TACE.

Keywords: hepatocellular carcinoma, recurrence, postoperative adjuvant transcatheter arterial chemoembolization, radiomics

Introduction

Hepatocellular carcinoma (HCC) is the sixth most prevalent malignancy and third leading cause of cancer-related death worldwide.[1] Due to the shortage of organ donor for liver transplantation, surgical resection remains the mainstay curative treatment option for HCC.[2] However, the long-term prognosis is still poor owing to the high incidence of HCC recurrence in 60~70% of patients within 5 years after curative surgery,[3–5] making it necessary to take postoperative adjuvant treatments into account.

It is recommended that HCC patients should receive postoperative adjuvant transcatheter arterial chemoembolization (PA-TACE) at 1–3 months after the initial operation when their liver function recovers to normal.[6] Specifically, PA-TACE

Received: 1 March 2022
Accepted: 9 May 2022
Published: 23 May 2022

was reported to benefit patients with certain high-risk recurrence factors including large tumor size, multi-nodularity, microscopic vascular invasion and macroscopic portal vein tumor thrombus (m-PVTT).[7–10] Theoretically, PA-TACE has been considered capable of eliminating intrahepatic micro-metastases or residual tumor foci to prevent recurrence and thus improve the prognosis.[11–13] However, the role of PA-TACE for resected HCC remains controversial in clinical practice. Several studies have found no obvious survival benefit or even a decline of recurrence-free survival (RFS) and overall survival (OS) in HCC patients within PA-TACE, which may be related to hepatic and immunological functions impairment by PA-TACE.[14,15] Hence, this study aids in exploring which patients with resected HCC could benefit from PA-TACE.

Recently, as an emerging technique in medical image processing, radiomics is used to convert medical images into mineable high-dimensional features which are related to the underlying tumor biology and clinical prognosis.[16,17] In other words, radiomics can help match quantitative image features that objectively reflect the potential biological characteristics of the tumor with the prognosis of patients. Moreover, CT-based radiomics has been proved to be an effective tool for predicting the recurrence of HCC after surgery.[18,19] However, no published research has focused on radiomics approaches for the added benefit of PA-TACE and in predicting RFS of HCC patients.

In this study, we aim to establish the recurrence risk model of HCC patients undergoing radical resection by CT-based radiomics features and validate by two independent cohorts, and further identify the patient subgroups that may benefit from PA-TACE.

Materials and Methods

Study Population

The review committees of the two medical institutions approved the study protocol and waived the requirement of informed consent from patients. This study was conducted in accordance with the Declaration of Helsinki. A total of 1192 patients with pathologically confirmed HCC who underwent radical resection were recruited from two independent institutions. And the exclusion criteria were as follows: (a) patient had received radiotherapy, chemotherapy, radio-frequency ablation, or other antitumor treatments before the operation, (b) CT scan was unavailable or performed over 1 month before surgery, (c) macrovascular invasion or extrahepatic metastasis was detected at the time of preoperative CT scan, (e) clinical-pathologic or follow-up data were missing. Finally, a total of 364 patients were included in the study. Two hundred and seventy-nine patients recruited from Institution I (Sir Run Run Shaw Hospital, Zhejiang University School of Medicine between February 2012 and December 2018) were randomly divided into training (n = 187) and internal validation (n = 92) cohorts. And 85 patients from institution II (The First Affiliated Hospital of Wenzhou Medical University between January 2016 and October 2019) formed the external validation cohort.

CT Imaging Examination

CT data acquisition and imaging parameters were listed in Table S1. All images were reconstructed into slice thickness of 5–7mm. The CT parameters were tube voltage of 120 kVp, tube current of 150–260 mAs, pixel spacing of 0.51–0.81 mm. The used nonionic contrast agents were Iohexol (Yangtze River Pharmaceutical Group, Taizhou, China) and Iodixanol and Iohexol (GE Healthcare Ireland, Carrigtwohill, Ireland). We used a high-pressure syringe (3.0–4.0 mL/s) to inject nonionic contrast agent (1.5–2.0 mL/kg), and CT scans of arterial phase and portal venous phase were performed at 15s and 70s after injection, respectively.

Clinical Data

Relevant clinical data included (a) demographics and clinical characteristics including age, gender, liver cirrhosis, etiology; (b) histologic characteristics including Edmondson-Steiner grade, microvascular invasion (MVI), (c) laboratory variables including alpha-fetoprotein (AFP), alanine aminotransferase (ALT), aspartate aminotransferase (AST), albumin (ALB), glutamyl transpeptidase (GGT), total bilirubin (TB), conjugated bilirubin (CB), platelet count (PLT), prothrombin time (PT), international normalized ratio (INR), and (d) several grading systems including Child-Pugh class, albumin-bilirubin (ALBI) grade,[20,21] Barcelona Clinic Liver Cancer (BCLC) staging system.[22]

Follow-Up

All patients were scheduled for re-examination 1–3 months after the initial operation, and the PA-TACE treatment strategy was recommended by the physician after liver function recovered. All patients were postoperatively followed up every 3–6 months during the first 2 years, every 6 months during the next 3 years, and then annually thereafter. When recurrence was suspected, enhanced computed tomography (CT) scan or magnetic resonance imaging (MRI) was performed. The endpoints of this study were recurrence-free survival (RFS), which was defined as the time from surgery to the recurrence or intrahepatic/extrahepatic metastasis or to the date of last follow-up.

Radiological Features Evaluation

Preoperative CT images were retrospectively evaluated using a Picture Archiving and Communication System (PACS) by two abdominal radiologists (doc1 and doc2, with 5- and 10-year experience in liver imaging, respectively). The two reviewers were not given the clinical information of the participants and then independently assessed the following imaging features, including tumor number, largest tumor size, tumor growth pattern, tumor margin, capsule appearance, intratumoral hemorrhage, intratumoral necrosis, arterial peritumoral enhancement, radiogenomic venous invasion (RVI). A joint review between two radiologists was performed to reach a consensus.

Radiomics Analysis

The same two radiologists were involved in the tumor segmentation on each transverse slice of pre-contrast, arterial and portal venous phase using ITK-SNAP software (version 3.8.0, www.itksnap.org). The tumor area was contoured manually by doc1 and a 10-mm-wide band was generated with automated dilation to capture radiomics features from the tumor periphery. A test-retest procedure was performed on 30 randomly selected patients, which were delineated again by doc1 and doc2 to investigate the reproducibility of extracted features by intra- and inter-class correlation coefficients (ICCs).

Image preprocessing and radiomics feature extraction were implemented with the open-source python Pyradiomics package (version 2.2.0, http://www.radiomics.io/pyradiomics.html). CT images from two institutions were resampled into isotropic resolution of $1.0 \times 1.0 \times 1.0 mm^3$ to eliminate the inconsistency of spatial resolution. Eight hundred and fifty-three features based on shape, intensity and texture were extracted from each three-dimensional segmentation region by using engineered hard-coded feature algorithm,[23] and a total of 5118 features for every lesion (tumor and peritumoral tissue in the pre-contrast, arterial and portal venous phase) were given.

Development and Validation of RFS-Predictive Models

All the radiomics features were normalized with z-scores. The intra- and inter-class correlation coefficients (ICCs) were calculated to measure the intra- and inter-rater reproducibility of the radiomics features, respectively. Features with ICCs less than 0.8 were removed. In the training cohort, univariable Cox proportional hazard regression analysis was first performed for each radiomics feature, features with p-value <0.05 were considered significantly related to recurrence. Next, five-fold cross validation and least absolute shrinkage and selection operator (LASSO) algorithms were applied to select optimal radiomics features. Finally, the radiomics model based on the selected radiomics features was established using the random survival forests method.[24] The participants were divided into high-risk signature (HRS) and low-risk signature (LRS) group according to the median value of radiomics score (Rad-score) calculated by the Radiomics model. The underlying correlation between the Rad-score and RFS was explored in the training cohort and verified in the both internal and external validation cohorts using Kaplan–Meier survival analysis. Additionally, the Clinical nomogram was constructed by independent clinical factors and the Combined nomogram was built using the Rad-score and the clinical risk factors, both models were used to predict RFS in all cohorts.

Statistical Analysis

To investigate the differences in demographic and clinical variables between the training and validation cohorts, Student's t-test or Mann–Whitney U-test was used for continuous variables, and Chi-square test or Fisher exact test was used for categorical variables.

In addition, univariate and multivariate Cox regression analyses were performed to identify the independent predictors of RFS. Survival curves were analyzed using the Kaplan–Meier method and compared by Log rank test. Time-dependent receiver operating characteristics (ROC) curves for 1-year, 2-year and 3-year RFS were plotted to evaluate the predictive accuracy of two risk groups. Harrell's concordance index (C-index), calibration curves and decision curve analysis were used to evaluate the predictive performance of the risk models.

Statistical analyses were carried out using R software with the "survival" and "rms" packages (version 4.0.3, http://www.r-project.org) and SPSS software (version 26.0, https://www.ibm.com). A $P < 0.05$ indicated a statistical significance.

Results

Patient Characteristics

The study design is described in Figure S1. The demographic and clinical characteristics of patients in the training, the internal, and external validation cohorts are summarized in Table 1, which showed the distribution of all clinical-radiologic-pathologic characteristics were similar across the training and the internal or external validation cohorts. The median follow-up durations were 28.0 (22.7–33.3), 29.0 (15.6–42.3) and 25.0 (19.7–30.3) months for the three cohorts, respectively.

Radiomics Analysis

Among the 5118 extracted radiomics features, 2422 features with ICCs > 0.80 were preliminarily selected. After applying univariable Cox proportional hazard regression analysis and LASSO algorithm, 81 features were retained and used to predict RFS based on the random survival forests method (Table S2). The significant difference in RFS between the HRS and LRS groups ($P < 0.001$) was confirmed by the Kaplan–Meier survival curves, with relatively high hazard ratios in the training (HRs > 13.021), the internal (HRs ≥ 5.413) and external validation (HRs ≥ 6.928) cohorts (Figure 1A). The time-dependent ROCs and AUCs at 1-, 2- and 3-year RFS in three cohorts are exhibited in Figure 1B, with AUCs of 0.913–0.942, 0.784–0.877, and 0.853–0.909 in the training, the internal and external validation cohorts, respectively. Furthermore, when the patients were sub-grouped by different BCLC stage (0-A or A1-B), such two risk stratifications remained as strong prognostic predictors, with all Log rank test $P < 0.05$ (Figure S2).

Comparison of RFS-Predictive Models

In the training cohort, 6 significant predictors, including the Rad-score and 5 clinic-pathological-radiologic characteristics such as MVI, arterial peritumoral enhancement, RVI, tumor size, and BCLC stage were statistically significant factors by univariate analysis (Table S3). Among them, two clinical features such as MVI and arterial peritumoral enhancement were selected by multivariate analysis as independent predictors of recurrence, which constituted the Clinical nomogram (Figure S3, Table S4), while only MVI and Rad-score were finally incorporated into the Combined nomogram (Figure 2A, Table S4). The C-index values for the three models are listed in Table 2, which demonstrated that Rad-score performed better in predicting RFS with C-index (95% CI) ranged from 0.809 (0.775–0.843) to 0.892 (0.877–0.907) than Clinical nomogram ranged from 0.670 (0.638–0.702) to 0.680 (0.636–0.724) among three cohorts. In addition, the Combined nomogram further improved accuracy for predicting RFS with C-index ranging from 0.830 (0.793–0.867) to 0.898 (0.884–0.912). The calibration curve of the Combined nomogram and the Clinical nomogram illustrated optimal agreement between the predicted and observed RFS among three cohorts (Figures 2B and S4). The decision curve analysis was performed to show that the Combined nomogram had relatively better clinical usefulness and faintly higher net benefits across almost the entire range of reasonable threshold probabilities (Figure 2C). The corresponding prediction error curves of all cox models are shown in Figure 3A–D, which further indicated that the Clinical nomogram was inferior to the Rad-score or the Combined nomogram for predicting RFS.

Benefit Prediction of PA-TACE

Eighteen patients were excluded from this study because they were found to have tumor recurrence during the first evaluation 1–3 months after surgery. Thus, 346 patients were included for PA-TACE analysis. For patients who received PA-TACE or not, the Rad-score alone was correlated with RFS in all patients (Figure 4A–B). Furthermore, HRS

Table 1 Comparison of Baseline Clinical-Radiologic-Pathologic Characteristics Among Three Cohorts

Characteristics		Training Cohort (n=187)	Internal Validation Cohort (n=92)	*P*	External Validation Cohort (n=85)	*P*
Age (mean (SD))		57.72 (11.05)	56.93 (12.20)	0.592	60.25 (10.88)	0.080
Gender	Male	166 (88.77)	75 (81.52)	0.141	73 (85.88)	0.634
	Female	21 (11.23)	17 (18.48)		12 (14.12)	
Liver cirrhosis	Yes	123 (65.78)	64 (69.57)	0.619	56 (65.88)	1.000
	No	64 (34.22)	28 (30.43)		29 (34.12)	
Etiology	HBV	139 (74.33)	67 (72.83)	0.901	69 (81.18)	0.280
	Other	48 (25.67)	25 (27.17)		16 (18.82)	
AFP, ng/mL	≤200	120 (64.17)	62 (67.39)	0.691	64 (75.29)	0.093
	>200	67 (35.83)	30 (32.61)		21 (24.71)	
ALT, U/mL	≤50	130 (69.52)	63 (68.48)	0.969	61 (71.76)	0.816
	>50	57 (30.48)	29 (31.52)		24 (28.24)	
AST, U/mL	≤40	112 (59.89)	61 (66.30)	0.365	51 (60.00)	1.000
	>40	75 (40.11)	31 (33.70)		34 (40.00)	
ALB, g/L	≤36	43 (22.99)	22 (23.91)	0.984	25 (29.41)	0.326
	>36	144 (77.01)	70 (76.09)		60 (70.59)	
GGT, U/L	≤45	86 (45.99)	37 (40.22)	0.433	39 (45.88)	1.000
	>45	101 (54.01)	55 (59.78)		46 (54.12)	
TB, μmol/L	≤19	103 (55.08)	53 (57.61)	0.786	57 (67.06)	0.084
	>19	84 (44.92)	39 (42.39)		28 (32.94)	
CB, μmol/L	≤6.8	140 (74.87)	66 (71.74)	0.679	59 (69.41)	0.428
	>6.8	47 (25.13)	26 (28.26)		26 (30.59)	
PLT, $\times 10^9$/L	≤100	50 (26.74)	27 (29.35)	0.752	19 (22.35)	0.535
	>100	137 (73.26)	65 (70.65)		66 (77.65)	
PT, seconds	≤13	53 (28.34)	27 (29.35)	0.973	17 (20.00)	0.190
	>13	134 (71.66)	65 (70.65)		68 (80.00)	
INR	≤1.0	39 (20.97)	24 (26.09)	0.420	11 (12.94)	0.158
	>1.0	147 (79.03)	68 (73.91)		74 (87.06)	
Child-Pugh grade	A	160 (85.56)	77 (83.70)	0.817	66 (77.65)	0.15
	B or C	27 (14.44)	15 (16.30)		19 (22.35)	
ALBI grade	1	104 (55.61)	44 (47.83)	0.272	43 (50.59)	0.522
	2 or 3	83 (44.39)	48 (52.17)		42 (49.41)	

(*Continued*)

Table 1 (Continued).

Characteristics		Training Cohort (n=187)	Internal Validation Cohort (n=92)	*P*	External Validation Cohort (n=85)	*P*
BCLC classification	0	37 (13.60)	10 (10.87)	0.775	11 (12.94)	0.137
	A	140 (51.47)	45 (48.91)		51 (60.00)	
	A1 or B	95 (34.93)	37 (40.22)		23 (27.06)	
MVI	Absent	111 (59.36)	47 (51.09)	0.237	52 (61.18)	0.881
	Present	76 (40.64)	45 (48.91)		33 (38.82)	
Edmondson grade	I	56 (29.95)	31 (33.70)	0.376	26 (30.59)	0.506
	II	87 (46.52)	46 (50.00)		34 (40.00)	
	III/IV	44 (23.53)	15 (16.30)		25 (29.41)	
Tumor size, cm	≤5.0	120 (64.17)	58 (63.04)	0.959	65 (76.47)	0.061
	>5.0	67 (35.83)	34 (36.96)		20 (23.53)	
Tumor number	Solitary	173 (92.51)	89 (96.74)	0.194	81 (95.29)	0.599
	Multiple	14 (7.49)	3 (3.26)		4 (4.71)	
Tumor growth pattern	Intrahepatic growth	156 (83.42)	78 (84.78)	0.907	76 (89.41)	0.268
	Extrahepatic growth	31 (16.58)	14 (15.22)		9 (10.59)	
Tumor margin	Smooth	70 (37.43)	37 (40.22)	0.750	36 (42.35)	0.524
	Non–smooth	117 (62.57)	55 (59.78)		49 (57.65)	
Capsule appearance	Incomplete	150 (80.21)	76 (82.61)	0.751	68 (80.00)	1.000
	Complete	37 (19.79)	16 (17.39)		17 (20.00)	
Intratumor hemorrhage	Absent	166 (88.77)	79 (85.87)	0.616	78 (91.76)	0.591
	Present	21 (11.23)	13 (14.13)		7 (8.24)	
Intratumoral necrosis	Absent	123 (65.78)	65 (70.65)	0.496	63 (74.12)	0.218
	Present	64 (34.22)	27 (29.35)		22 (25.88)	
Arterial peritumoral enhancement	Absent	147 (78.61)	72 (78.26)	1.000	72 (84.71)	0.312
	Present	40 (21.39)	20 (21.74)		13 (15.29)	
Radiogenomic venous invasion	Negative	109 (58.29)	54 (58.70)	0.504	51 (60.00)	0.661
	Positive	78 (41.71)	38 (41.30)		34 (40.00)	
Recurrence	Median time [IQR]	28.0[22.7, 33.3]	29.0[15.6, 42.3]	0.333	25.0 [19.7, 30.3]	0.713
No. of recurrences		79 (42.25)	39 (42.39)	1.000	30 (35.29)	0.342

Abbreviations: SD, standard deviation; AFP, alpha-fetoprotein; ALT, alanine aminotransferase; AST, aspartate aminotransferase; ALB, albumin; GGT, glutamyl transpeptidase; TB, total bilirubin; CB; conjugated bilirubin; PLT, platelet count; PT, prothrombin time; INR, international normalized ratio; ALBI, albumin-bilirubin; BCLC, Barcelona Clinic Liver Cancer; MVI, microvascular invasion; IQR, interquartile range.

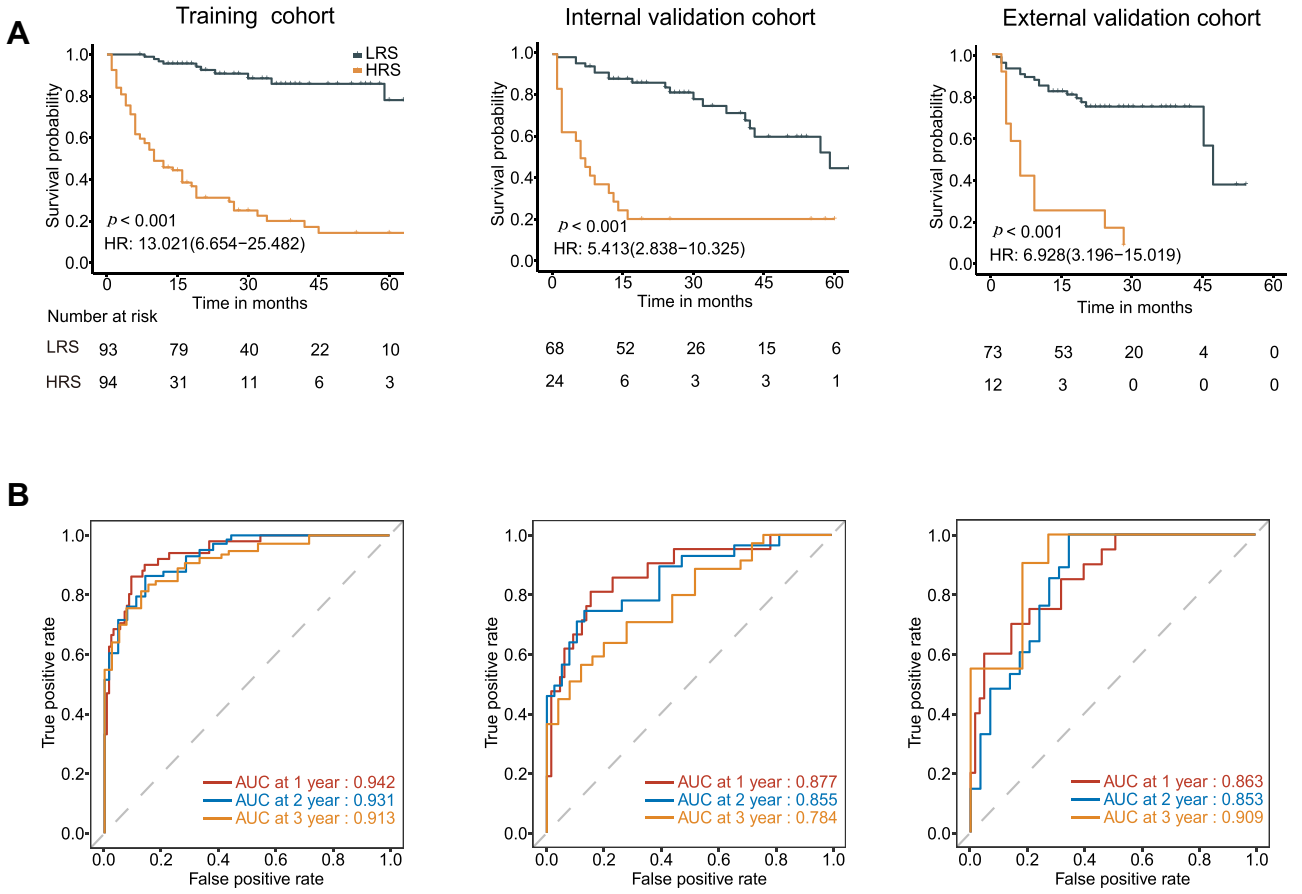

Figure 1 Kaplan-Meier survival analysis and time-dependent ROC curves based on Rad-score. (**A**) Kaplan-Meier survival analysis based on Rad-score. (**B**) The time-dependent ROC curves according to Rad-score. *P* values were calculated using the Log rank test, and AUCs at 1, 2 and 3 years were used to assess the prognostic accuracy within the training, the internal and external validation cohorts.

Abbreviations: Rad-score, radiomics score; AUC, area under the curve; HR, hazard ratio; ROC, receiver operating characteristic; LRS, low radiomics score; HRS, high radiomics score.

appeared to be more closely related to the RFS of HCC patients. A test for an interaction between Rad-score and PA-TACE indicated that compared with patients in the LRS group (HR: 0.693, 95% CI: 0.390–1.231, $P = 0.210$), the PA-TACE benefited greater in patients with HRS (HR: 0.085, 95% CI: 0.042–0.170, $P < 0.001$; $P < 0.001$ for interaction, Table 3). The corresponding Kaplan-Meier RFS curves were plotted to compare the LRS and HRS (Figure 4C–D). We found that PA-TACE significantly increased RFS in the HRS group ($P < 0.001$), but no significant value for the LRS group ($P = 0.210$).

Discussion

The aim of this study, besides developing and validating a recurrence risk model based on CT radiomics features for HCC patients, is to investigate the correlation between the Rad-score and PA-TACE. The radiomics model exhibited superior prognostic performance compared with the Clinical nomogram built using traditional clinical-radiologic-pathologic characteristics. Moreover, stratification based on Rad-score can identify patients who can benefit from PA-TACE.

It is known that HCC is an extremely heterogenous malignant tumor, the clinical results showed significant differences even among patients who receive similar treatment at the same stage.[25] Gene signatures obtained from single-gene or multi-gene expression profiles and next-generation sequencing might be available biomarkers that reflect biological behavior, which was indicated to be related to HCC prognosis.[26] Unfortunately, due to its exorbitant cost and invasiveness, it is not used in routine clinical practice. Thus, our study aims to explore a non-invasive and easy-to-use tool to predict HCC recurrence. Several recent studies have demonstrated the prognostic value of radiomics features

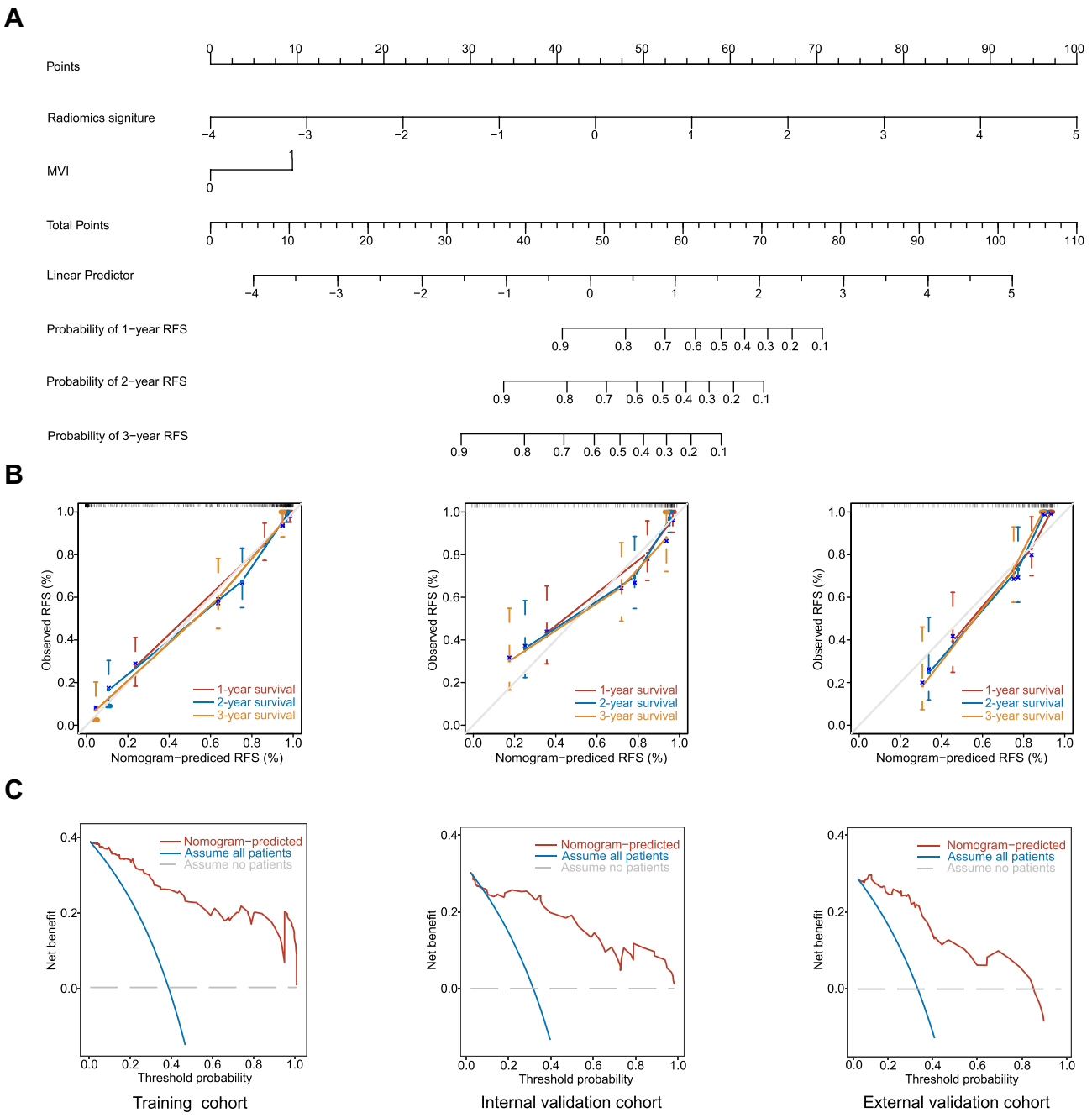

Figure 2 Combined nomogram used to estimate RFS for HCC, along with the calibration curves and decision curves for the Combined nomogram. (**A**) The Combined nomogram for RFS. (**B**) The calibration curves for the Combined nomogram in the training, the internal and external validation cohorts. (**C**) The decision curves for the Combined nomogram in the training, the internal and external validation cohorts.
Abbreviations: RFS, recurrence-free survival; MVI, microvascular invasion.

in HCC.[18,19,27,28] The findings may be attributed to the fact that radiomics can identify subtle differences in both intensity and texture which are not easily detectable by human eyes and can comprehensively characterize the tumor phenotype by high throughput extraction of numerous quantitative medical imaging features.[16,17] In our study, multi-phase CT radiomics features were used to establish the radiomics model to predict RFS successfully, with a C-index of 0.892, 0.812, 0.809 in the training, the internal and external validation cohorts, respectively.

In addition, MVI was found to be one of the most important prognostic factors of HCC in both Clinical nomogram and Combined nomogram, which was in line with the previous studies.[18–20,29] As an additional significant marker of

Table 2 The Performances of the Different Models in the Training and Validation Cohorts

Cohort	C-Index (95% CI)		
	Rad-Score	Clinical Nomogram	Combined Nomogram
Training cohort	0.892 (0.877–0.907)	0.670 (0.638–0.702)	0.898 (0.884–0.912)
Internal validation cohort	0.812 (0.776–0.848)	0.673 (0.635–0.711)	0.830 (0.793–0.867)
External validation cohort	0.809 (0.775–0.843)	0.680 (0.636–0.724)	0.835 (0.804–0.866)

Abbreviations: Rad-score, radiomics score; CI, confidence interval.

histologic MVI,[27,30,31] arterial peritumoral enhancement was also found to be one independent clinical factor for HCC prognosis. Of note, incorporating Rad-score into clinical-radiologic-pathologic information could add some prognostic information to better predict the recurrence risk of HCC patients. Furthermore, we found that the Combined nomogram improved the prognostic ability of the clinical factors and exhibited comparable performance to the Radiomics model. Given the excellent prediction performance of both Rad-score and Combined nomogram, we used lightweight and flexible Rad-score to analyze further.

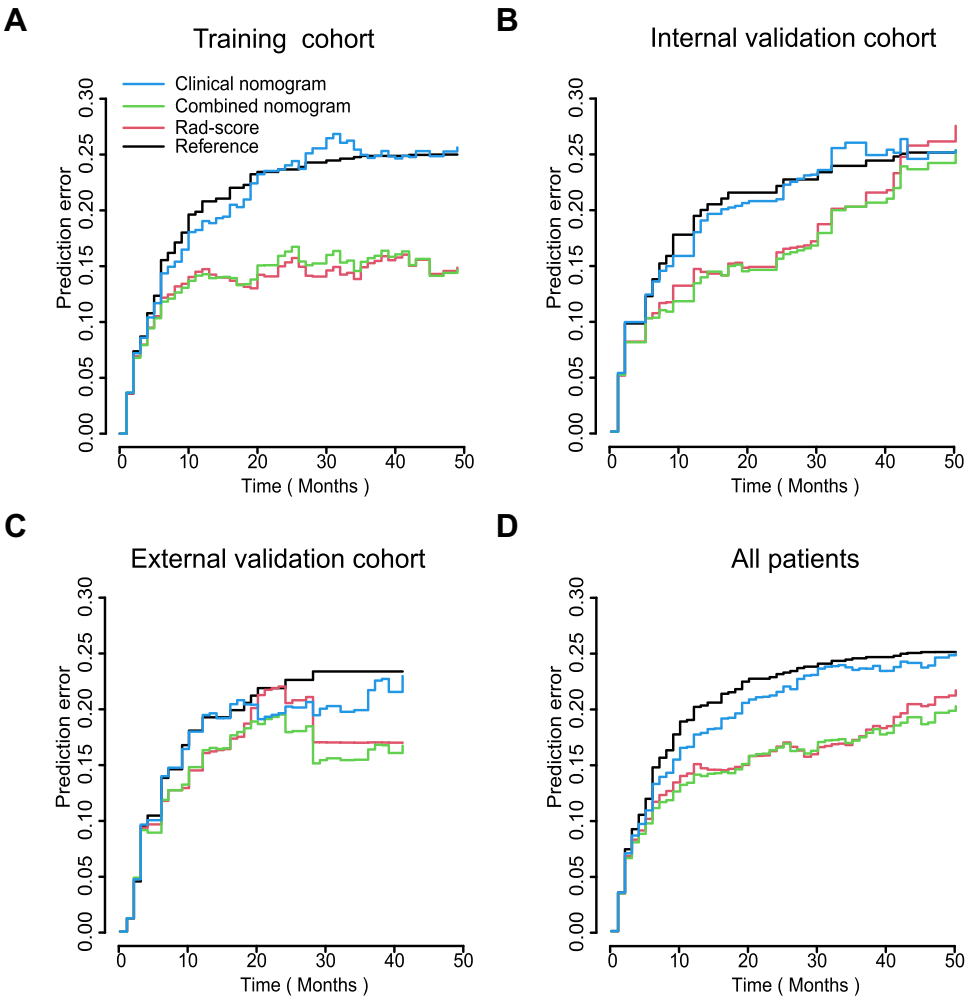

Figure 3 Prediction error curves for each model in stratifying RFS among the training, the internal and external validation cohorts. Prediction error curves for the (**A**) training cohort, the (**B**) internal validation cohort, the (**C**) external validation cohort and the (**D**) all patients. The lower prediction errors portend higher model accuracy.
Abbreviations: Rad-score, radiomics score; RFS, recurrence-free survival.

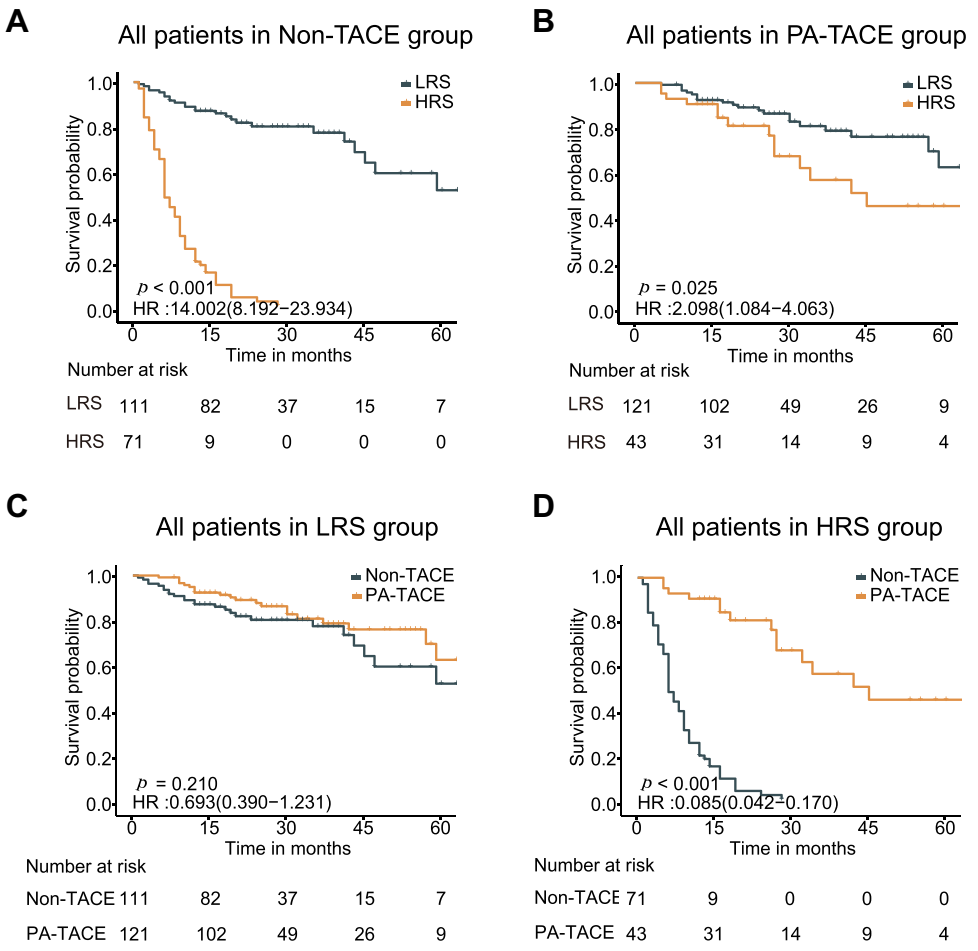

Figure 4 The Kaplan-Meier analysis curves used for the assessment PA-TACE benefits. (**A**) Non-TACE patients. (**B**) PA-TACE patients. (**C**) LRS patients. (**D**) HRS patients. P values were calculated using the Log rank test.

Abbreviations: RFS, recurrence-free survival; PA-TACE, postoperative adjuvant transcatheter arterial chemoembolization; Non-TACE, without postoperative adjuvant transcatheter arterial chemoembolization; HR, hazard ratio; LRS, low radiomics score; HRS, high radiomics score.

Our radiomics model is a powerful and externally validated tool to predict tumor recurrence, which could be used to stratify patients into subgroups with high and low risk of recurrence. This approach might provide an unprecedented opportunity to improve clinical decision support for patients with HCC after resection. Surgical resection alone appeared sufficient for the LRS group, while for patients with HRS, additional PA-TACE should be considered.[9,10,13,26] Although previous studies have confirmed that PA-TACE was an effective treatment for HCC patients after resection to reduce recurrence and improve survival, some investigators believed that only a subset of patients could benefit from PA-TACE.[11–15] Interestingly, in the present study, PA-TACE benefited greater in HCC patients within HRS group. For the LRS group, PA-TACE only slightly improved prognosis, which was similar to the previous studies.[7,8,13,32] Recently, CT radiomics features

Table 3 Treatment Interaction with Radiomics Score for Recurrence Free Survival in Patients with HCC

Rad-Score	PA-TACE	Non-TACE	PA-TACE VS Non-TACE, HR (95% CI)	*P*	*P* value for Interaction
All patients					<0.001
LRS	121	111	0.693 (0.390–1.231)	0.210	
HRS	43	71	0.085 (0.042–0.170)	<0.001	

Abbreviations: Rad-score, radiomics score; PA-TACE, postoperative adjuvant transcatheter arterial chemoembolization; Non-TACE, without postoperative adjuvant transcatheter arterial chemoembolization; HR, hazard ratio; LRS, low radiomics score; HRS, high radiomics score.

and clinical factors had been applied to achieve excellent performance in predicting the first TACE response in intermediate-stage HCC patients.[33] Herein, we identified that PA-TACE provided a better survival benefit to HCC patients in the HRS group. Thus, the use of a Rad-score enabled more accurate identification of patients who are likely to benefit from PA-TACE. In patients with LRS, an appropriate therapeutic strategy needs to be further explored to improve the prognostic performance. The concrete mechanisms of the relationship between radiomics features and PA-TACE have not been thoroughly investigated. It is probably due to the fact that PA-TACE can eliminate intrahepatic micro-metastases, residual small foci, or cancer cells dissociated by surgical extrusion, which can be detected by radiomics within sufficient discriminatory power.[11,12,34]

Despite the importance of the developed model, this study has several limitations. Firstly, it was a retrospective study with relatively small samples; the models would be improved if trained and validated in larger well-designed prospective studies. Second, the subjects in our study are China populations with hepatitis B viral infection, which may lead to etiology-based differences. Thus, this model should be validated in a Western cohort, where alcoholic liver disease and hepatitis C viral infection are more common. Third, multi-phase MRI has been widely used in HCC diagnosis without invasive biopsies, which should be further considered. Fourth, digital biopsy, pathological imaging, and genomic sequencing were not investigated in our study, which may provide more micro information for HCC prognosis. Finally, deep learning, a promising method that can automatically learn feature representations from images according to clinical goals and without manual segmentation by experienced radiologists, merits further exploration.

Conclusion

We developed a CT-based Rad-score that can effectively predict RFS for patients with resected HCC and provide additional prognostic value to the traditional clinical-radiologic-pathologic prediction model. Moreover, the Rad-score might be a useful predictive tool to explore patient who could benefit from PA-TACE. These results warrant further validation in future randomized trials to test the clinical utility of our imaging signature in combination with clinical-radiologic-pathologic criteria to guide individualized therapeutic selection.

Abbreviations

HCC, hepatocellular carcinoma; RFS, recurrence-free survival; Rad-score, radiomics score; PA-TACE, postoperative adjuvant transcatheter arterial chemoembolization; Non-TACE, without postoperative adjuvant transcatheter arterial chemoembolization; HR, hazard ratio; CI, confidence interval; C-index, concordance index; SD, standard deviation; IQR, interquartile range; LRS, low radiomics score; HRS, high radiomics score; AFP, alpha-fetoprotein; ALT, alanine aminotransferase; AST, aspartate aminotransferase; ALB, albumin; GGT, glutamyl transpeptidase; TB, total bilirubin; CB; conjugated bilirubin; PLT, platelet count; PT, prothrombin time; INR, international normalized ratio; ALBI, albumin-bilirubin; BCLC, Barcelona Clinic Liver Cancer; MVI, microvascular invasion.

Ethics Approval and Informed Consent

The study protocols were approved by the ethics committees of Sir Run Run Shaw Hospital, Zhejiang University School of Medicine and The First Affiliated Hospital of Wenzhou Medical University. A waiver of informed consent was granted due to the retrospective data collection. All patient data accessed complied with relevant data protection and privacy regulations.

Author Contributions

All authors had full access to the conception, study design, execution, acquisition of data, analysis and interpretation of the data, or in all these areas; substantially contributed to drafting, revising, or critically reviewing the article; approved the final version of the report to be published; agreed on the journal to which the essay has been submitted; and agreed to be accountable for all aspects of the work.

Funding

This study was supported by the National Natural Science Foundation of China (82071988), the Key Research and Development Program of Zhejiang Province (2019C03064), the Program Co-sponsored by Province and Ministry

(No.WKJ-ZJ-1926) and the Special Fund for Basic Scientific Research Business Expenses of Zhejiang University (No.2021FZZX003-02-17).

Disclosure

The authors have no competing interests to declare in this work.

References

1. Sung H, Ferlay J, Siegel RL, et al. Global cancer statistics 2020: GLOBOCAN estimates of incidence and mortality worldwide for 36 cancers in 185 countries. *CA Cancer J Clin*. 2021;71(3):209–249. doi:10.3322/caac.21660
2. Kanwal F, Befeler A, Chari RS, et al. Potentially curative treatment in patients with hepatocellular cancer–results from the liver cancer research network. *Aliment Pharmacol Ther*. 2012;36(3):257–265. doi:10.1111/j.1365-2036.2012.05174.x
3. Imamura H, Matsuyama Y, Tanaka E, et al. Risk factors contributing to early and late phase intrahepatic recurrence of hepatocellular carcinoma after hepatectomy. *J Hepatol*. 2003;38(2):200–207. doi:10.1016/S0168-8278(02)00360-4
4. Tung-Ping Poon R, Fan ST, Wong J. Risk factors, prevention, and management of postoperative recurrence after resection of hepatocellular carcinoma. *Ann Surg*. 2000;232(1):10–24. doi:10.1097/00000658-200007000-00003
5. Xu XF, Xing H, Han J, et al. Risk factors, patterns, and outcomes of late recurrence after liver resection for hepatocellular carcinoma: a multicenter study from China. *JAMA Surg*. 2019;154(3):209–217. doi:10.1001/jamasurg.2018.4334
6. Wang H, Du PC, Wu MC, Cong WM. Postoperative adjuvant transarterial chemoembolization for multinodular hepatocellular carcinoma within the Barcelona clinic liver cancer early stage and microvascular invasion. *Hepatobiliary Surg Nutr*. 2018;7(6):418–428. doi:10.21037/hbsn.2018.09.05
7. Ren ZG, Lin ZY, Xia JL, et al. Postoperative adjuvant arterial chemoembolization improves survival of hepatocellular carcinoma patients with risk factors for residual tumor: a retrospective control study. *World J Gastroenterol*. 2004;10(19):2791–2794. doi:10.3748/wjg.v10.i19.2791
8. Chen X, Zhang B, Yin X, Ren Z, Qiu S, Zhou J. Lipiodolized transarterial chemoembolization in hepatocellular carcinoma patients after curative resection. *J Cancer Res Clin Oncol*. 2013;139(5):773–781. doi:10.1007/s00432-012-1343-7
9. Zhong JH, Li LQ. Postoperative adjuvant transarterial chemoembolization for participants with hepatocellular carcinoma: a meta-analysis. *Hepatol Res*. 2010;40(10):943–953. doi:10.1111/j.1872-034X.2010.00710.x
10. Zhong JH, Ma L, Li LQ. Postoperative therapy options for hepatocellular carcinoma. *Scand J Gastroenterol*. 2014;49(6):649–661. doi:10.3109/00365521.2014.905626
11. Sun JJ, Wang K, Zhang CZ, et al. Postoperative adjuvant transcatheter arterial chemoembolization after R0 hepatectomy improves outcomes of patients who have hepatocellular carcinoma with microvascular invasion. *Ann Surg Oncol*. 2016;23(4):1344–1351. doi:10.1245/s10434-015-5008-z
12. Li F, Guo Z, Zhang Y, et al. Postoperative adjuvant arterial chemoembolization improves the survival of hepatitis B virus-related hepatocellular carcinoma: a retrospective control study. *Ir J Med Sci*. 2015;184(4):753–759. doi:10.1007/s11845-014-1164-6
13. Wang Z, Ren Z, Chen Y, et al. Adjuvant transarterial chemoembolization for HBV-related hepatocellular carcinoma after resection: a randomized controlled study. *Clin Cancer Res*. 2018;24(9):2074–2081. doi:10.1158/1078-0432.CCR-17-2899
14. Qi YP, Zhong JH, Liang ZY, et al. Adjuvant transarterial chemoembolization for patients with hepatocellular carcinoma involving microvascular invasion. *Am J Surg*. 2019;217(4):739–744. doi:10.1016/j.amjsurg.2018.07.054
15. Lai EC, Lo CM, Fan ST, Liu CL, Wong J. Postoperative adjuvant chemotherapy after curative resection of hepatocellular carcinoma: a randomized controlled trial. *Arch Surg*. 1998;133(2):183–188. doi:10.1001/archsurg.133.2.183
16. Aerts HJ, Velazquez ER, Leijenaar RT, et al. Decoding tumour phenotype by non-invasive imaging using a quantitative radiomics approach. *Nat Commun*. 2014;5:4006. doi:10.1038/ncomms5006
17. Gillies RJ, Kinahan PE, Hricak H. Radiomics: images are more than pictures, they are data. *Radiology*. 2016;278(2):563–577. doi:10.1148/radiol.2015151169
18. Ji GW, Zhu FP, Xu Q, et al. Radiomic features at contrast-enhanced CT predict recurrence in early stage hepatocellular carcinoma: a multi-institutional study. *Radiology*. 2020;294(3):568–579. doi:10.1148/radiol.2020191470
19. Ji GW, Zhu FP, Xu Q, et al. Machine-learning analysis of contrast-enhanced CT radiomics predicts recurrence of hepatocellular carcinoma after resection: a multi-institutional study. *EBioMedicine*. 2019;50:156–165. doi:10.1016/j.ebiom.2019.10.057
20. Chan AWH, Zhong J, Berhane S, et al. Development of pre and post-operative models to predict early recurrence of hepatocellular carcinoma after surgical resection. *J Hepatol*. 2018;69(6):1284–1293. doi:10.1016/j.jhep.2018.08.027
21. Johnson PJ, Berhane S, Kagebayashi C, et al. Assessment of liver function in patients with hepatocellular carcinoma: a new evidence-based approach-the ALBI grade. *J Clin Oncol*. 2015;33(6):550–558. doi:10.1200/JCO.2014.57.9151
22. Tsilimigras DI, Bagante F, Sahara K, et al. Prognosis after resection of Barcelona Clinic Liver Cancer (BCLC) stage 0, A, and B hepatocellular carcinoma: a comprehensive assessment of the current BCLC classification. *Ann Surg Oncol*. 2019;26(11):3693–3700. doi:10.1245/s10434-019-07580-9
23. van Griethuysen JJM, Fedorov A, Parmar C, et al. Computational radiomics system to decode the radiographic phenotype. *Cancer Res*. 2017;77(21):e104–e107. doi:10.1158/0008-5472.CAN-17-0339
24. Ishwaran H, Kogalur UB, Blackstone EH, Lauer MS. Random survival forests. *Ann Appl Stat*. 2008;2(3):841–860. doi:10.1214/08-AOAS169
25. Forner A, Reig M, Bruix J. Hepatocellular carcinoma. *The Lancet*. 2018;391(10127):1301–1314. doi:10.1016/S0140-6736(18)30010-2
26. Villanueva A. Hepatocellular carcinoma. *N Engl J Med*. 2019;380(15):1450–1462. doi:10.1056/NEJMra1713263
27. Xu X, Zhang HL, Liu QP, et al. Radiomic analysis of contrast-enhanced CT predicts microvascular invasion and outcome in hepatocellular carcinoma. *J Hepatol*. 2019;70(6):1133–1144. doi:10.1016/j.jhep.2019.02.023
28. Kim S, Shin J, Kim DY, Choi GH, Kim MJ, Choi JY. Radiomics on gadoxetic acid-enhanced magnetic resonance imaging for prediction of postoperative early and late recurrence of single hepatocellular carcinoma. *Clin Cancer Res*. 2019;25(13):3847–3855. doi: 10.1158/1078-0432.CCR-18-2861
29. Miao W, Nie P, Yang G, et al. An FDG PET/CT metabolic parameter-based nomogram for predicting the early recurrence of hepatocellular carcinoma after liver transplantation. *Eur J Nucl Med Mol Imaging*. 2021;48(11):3656–3665. doi:10.1007/s00259-021-05328-w

30. Hong SB, Choi SH, Kim SY, et al. MRI features for predicting microvascular invasion of hepatocellular carcinoma: a systematic review and meta-analysis. *Liver Cancer*. 2021;10(2):94–106. doi:10.1159/000513704
31. Lee S, Kang TW, Song KD, et al. Effect of microvascular invasion risk on early recurrence of hepatocellular carcinoma after surgery and radiofrequency ablation. *Ann Surg*. 2021;273(3):564–571. doi:10.1097/SLA.0000000000003268
32. Liang L, Li C, Diao YK, et al. Survival benefits from adjuvant transcatheter arterial chemoembolization in patients undergoing liver resection for hepatocellular carcinoma: a systematic review and meta-analysis. *Therap Adv Gastroenterol*. 2020;13:1756284820977693. doi:10.1177/1756284820977693
33. Chen M, Cao J, Hu J, et al. Clinical-radiomic analysis for pretreatment prediction of objective response to first transarterial chemoembolization in hepatocellular carcinoma. *Liver Cancer*. 2021;10(1):38–51. doi:10.1159/000512028
34. Kubo S, Takemura S, Sakata C, Urata Y, Uenishi T. Adjuvant therapy after curative resection for hepatocellular carcinoma associated with hepatitis virus. *Liver Cancer*. 2013;2(1):40–46. doi:10.1159/000346214